

# Strength and deformability of small-scale rock mass models under large confinements

Saisuree Thaweboon<sup>1</sup> · Ronnachai Dasri<sup>1</sup> · Suratwadee Sartkaew<sup>1</sup> · Kittitep Fuenkajorn<sup>1</sup>

Received: 8 November 2015 / Accepted: 19 March 2016 / Published online: 4 April 2016  
© Springer-Verlag Berlin Heidelberg 2016

**Abstract** Triaxial compression tests were performed to determine the strength and deformability of small-scale rock mass models with multiple joint sets and frequencies under confining stresses up to 12 MPa. The cubical sandstone specimens ( $80 \times 80 \times 80 \text{ mm}^3$ ) with joint sets simulated by saw-cut surfaces were compressed to failure using a true triaxial load frame. The joint frequencies ranged from 26 to 76 joints per meter. The results indicate that the Hoek–Brown criterion with two material parameters ( $m$  and  $s$ ) can describe rock mass strengths as well as the three parameter criteria of Sheorey, Yudhbir and Ramamurthy-Arora. The parameter  $s$  notably decreases with increasing joint frequency, while parameter  $m$  is less sensitive to joint frequency. The confining stresses tend to enhance the effects of joint frequencies on rock mass compressive strengths. The deformation moduli in the direction normal to the joints tend to be lower than those parallel to the joints. They decrease with increasing joint frequency. Goodman's equation was modified here to allow calculation of the deformation moduli of the rock mass along the three principal directions. The modified equation can sufficiently describe the deformation moduli normal and parallel to the joints for one-joint set and three-joint set specimens under all confining stresses.

**Keywords** Triaxial compression · Joint frequency · Deformation modulus · Rock mass strength criterion

## Introduction

Several criteria have been proposed to describe rock mass strength based on laboratory testing (Hoek and Brown 1980; Saroglou and Tsiambaos 2008; Singh and Singh 2012; Rafiai 2011; Kulatilake et al. 2006). Some criteria are developed based on case studies (Sheorey et al. 1989; Cai et al. 2004) and numerical simulations (Halakatevakis and Sofianos 2010), primarily to determine the effects of joint frequency, joint orientation, and joint set number on rock mass strengths. It has been found that rock mass strength decreases with increasing joint frequency (Ramamurthy and Arora 1994) and joint set number (Yang et al. 1998). The joint orientation also affects rock mass strength. The lower strengths are obtained when the joint planes make angles between  $30^\circ$  and  $40^\circ$  with the major principal stress (Ramamurthy and Arora 1994; Colak and Unlu 2004; Goshtasbi et al. 2006). Some strength criteria have been verified by comparison with actual in-situ conditions (Edelbro 2004) and laboratory testing (Sridevi and Sitharam 2000; Goshtasbi et al. 2006).

Goodman (1970) presents an equation to evaluate the elastic constants for an equivalent continuous material representative of a rock mass regularly crossed by a single set of joints using the concept of joint stiffness. Based on testing results, Yoshinaka and Yamabe (1986) present equations for obtaining equivalent deformation moduli of rock masses with joints in arbitrary orientations and spacings. Ramamurthy (2001) introduces a joint factor to predict the decrease of deformation modulus with increasing joint frequency. The variation of the deformation moduli due to various joint orientations exhibits U-shaped behavior as reported by Ramamurthy (2001) and Tiwari and Rao (2006). Nasser et al. (2003), Tiwari and Rao (2006), and Ebadi et al. (2011) suggest that the deformation modulus tends to increase with confining pressure. Even though

✉ Kittitep Fuenkajorn  
kittitep@sut.ac.th

<sup>1</sup> Geomechanics Research Unit, Institute of Engineering, Suranaree University of Technology, Muang District, Nakhon Ratchasima 30000, Thailand

several rock mass strength and deformability criteria have been proposed, verification of their predictability under large confinements has rarely been attempted, particularly for rock masses with multiple joint sets.

The objective of this study was to perform triaxial compressive strength tests on sandstone specimens with single and multiple joint sets under confining stresses up to 12 MPa. The joints were simulated by saw-cut surfaces with frequencies ranging from 26 to 76 joints per meter. Some commonly used strength and deformability criteria were applied to the test results to evaluate their validity. From our results, the effects of joint frequency, joint set number, and confining stress on the strengths and deformation moduli of the small-scale rock mass models were determined.

### Sample preparation

The rock specimens used in this study were Phra Wihan sandstone, which is a fine-grained quartz sandstone with highly uniform texture and density (Boonsener and

Sonpiron 1997). We prepared them to obtain cubical rock mass specimens with nominal dimensions of  $80 \times 80 \times 80 \text{ mm}^3$ . We also made artificial joints out of saw-cut surfaces using a universal masonry saw (Husqvarna TS 400 F). This saw has a 400-mm diameter blade with a constant rotational speed of 2800 rpm. Water is used as cutting fluid. The saw base has two mutually perpendicular guide rails to provide a precise cutting angle and intervals. For our research, large blocks ( $250 \times 250 \times 250 \text{ mm}^3$ ) of the sandstone were first cut into thin slabs to obtain a predefined thickness (e.g., 40, 27, 20 and 13 mm) depending on the required joint frequencies. These slabs are then cut across to obtain tabular-shaped specimens, and subsequently, cubical-shaped specimens. These small blocks were assembled to form rock mass models with different joint frequencies and joint set numbers. Figure 1 shows example of rock blocks prepared for three-joint set specimens. Rock blocks with visible crack or chipping at the edges and corners were discarded. In total, we prepared up to 80 rock mass model specimens with two different joint conditions: single-joint set and sets with three mutually perpendicular joints. The joint frequencies and orientations with respect to the applied loads are shown in Table 1. They are briefly described below.

For case I, one-joint set specimens were prepared to study the effects of joint frequency on the strength of the rock specimens. The joints were parallel to the major principal axis. There were 1, 2, 3, or 4 joints for each set (equivalent to 26–63 joints per meter), and each set had equal spacing.

Case II is similar to case I: one-joint set specimens were prepared to assess the effect of joint frequency when the joints are normal to the major principal axis.

For Case III, specimens with three-mutually perpendicular joint sets were prepared to study the effects of joint

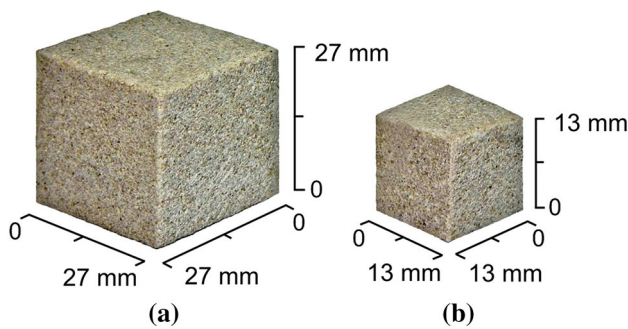


**Fig. 1** Examples of small blocks prepared for three-joint set specimens with 38 joints/m (a) and 76 joints/m (b)

**Table 1** Small-scale rock mass specimens prepared for triaxial compression tests with  $\sigma_3$  up to 12 MPa

Cases	Joint orientation	Joint frequencies (joints/m)				
		26	38	51	63	76
I	One-joint set parallel to the major principal axis					N/A
II	One-joint set normal to the major principal axis					N/A
III	Three-mutually perpendicular joint sets					

set number and joint frequency. This case involved 1, 2, 3, 4, or 5 joints for each set (equivalent to 26–76 joints per meter).

## Test method

A true triaxial load frame (Komenthammasopon 2014) was used to apply axial stress ( $\sigma_1$ ) and constant confining pressures ( $\sigma_3$ ) to the intact and jointed rock specimens (Fig. 2). This device was developed to test rock specimens with soft to medium strengths under polyaxial stress states. Three pairs of 100-ton hydraulic pressure cylinders are set in three mutually perpendicular directions. The measurement system comprises pressure transducers, displacement transducers, a switching box, and a data logger. The device can accommodate the cubic or rectangular specimens of different sizes by adjusting the distances between the opposite steel loading platens. For this study the specimens were oven-dried before testing. Neoprene sheets were placed at all interfaces between the loading platens and specimen surfaces to minimize the friction. The constant confining (lateral) stresses ranged from 0, 1, 3, 5, 7, to 12 MPa. First, the specimen was subjected to the pre-defined confining stresses. The axial stress was then increased at a constant rate of 0.1 MPa/s using an electric hydraulic pump. The specimen deformations were monitored along the three loading directions, and were used to calculate the principal strains during loading. The readings were recorded until failure occurred. We defined failure by the drop of the applied axial stress. Photographs were taken of the post-test specimens and the modes of failure were identified.

## Test results

Tables 2, 3, and 4 give the strength results in terms of the major and minor principal stresses at failure for cases I, II and III. The strengths decrease with increasing joint frequency.

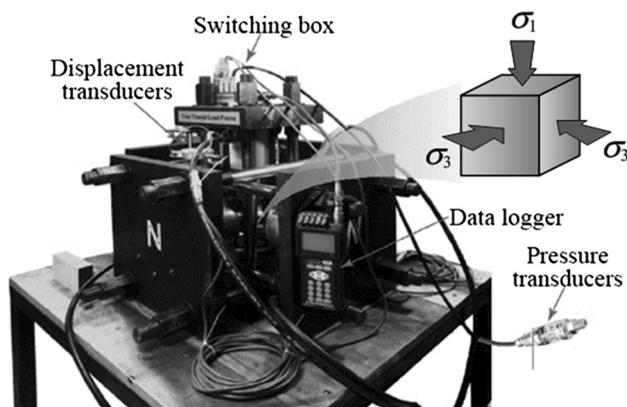


Fig. 2 True triaxial load frame

Table 2 Deformation moduli for case I

Joint frequency, $J_f$ (joints/m)	$\sigma_3$ (MPa)	$\sigma_1$ (MPa)	$\nu$	$E_{m,p}$ (GPa)	$E_{m,n}$ (GPa)	$E_{m,n}$ (GPa)
Intact	0	43.3	0.26	10.4	10.0	9.8
	1	47.8	0.28	10.3	10.3	10.3
	3	63.4	0.28	9.1	10.3	8.1
	5	74.1	0.27	10.7	10.1	11.5
	7	88.9	0.28	8.5	8.2	8.9
	12	106.9	0.27	9.7	10.4	9.2
26	0	36.1	0.27	7.7	7.7	7.7
	1	43.1	0.25	7.9	7.8	7.8
	3	59.0	0.26	5.5	5.5	4.6
	5	68.8	0.27	7.0	6.9	6.2
	7	77.6	0.25	6.2	6.4	6.0
	12	95.1	0.29	7.0	6.9	6.3
38	0	34.1	0.24	5.0	5.1	4.5
	1	41.1	0.27	5.1	5.2	4.5
	3	54.7	0.24	5.2	5.0	4.0
	5	66.0	0.24	5.3	5.2	5.1
	7	74.5	0.24	5.0	5.0	4.6
	12	91.0	0.27	6.2	5.9	5.8
51	0	29.0	0.24	3.1	3.2	3.0
	1	36.6	0.27	4.9	5.0	3.7
	3	51.3	0.28	5.1	5.1	5.0
	5	64.7	0.28	4.7	4.5	3.9
	7	70.5	0.25	5.4	5.5	5.4
	12	87.4	0.26	5.9	5.9	5.7
63	0	26.5	0.24	3.4	3.5	3.1
	1	34.8	0.23	3.8	3.6	2.8
	3	49.0	0.22	4.8	4.5	3.6
	5	59.4	0.24	4.4	4.4	4.3
	7	66.9	0.25	4.1	4.1	4.0
	12	82.9	0.29	4.2	4.2	4.2

Figure 3 shows examples of stress–strain relations in terms of the differential stress as a function of strain for the three mutually perpendicular joint set specimens (Case III). The effect of joint frequency on the rock specimens can be observed by the reduction of failure stresses and the increase of the failure strains. More discussions and analyses of the deformation moduli as affected by the joint frequency are given in the following section.

The effects of the confining stresses on the strength of the specimens can be observed from the  $\sigma_1$ – $\sigma_3$  diagrams, as shown in Fig. 4. The relations between  $\sigma_1$  and  $\sigma_3$  at failure tend to be non-linear for the intact sandstone and for the specimens with all joint frequencies. The specimens with higher joint frequencies ( $J_f$ ) show lower strengths than those with lower joint frequencies. The effect of joint frequency on strength tends to be greater for the specimens with joints parallel to  $\sigma_1$  (Case I, Fig. 4a), as compared to those with

**Table 3** Deformation moduli for case II

Joint frequency, $J_f$ (joints/m)	$\sigma_3$ (MPa)	$\sigma_1$ (MPa)	$\nu$	$E_{m,p}$ (GPa)	$E_{m,p}$ (GPa)	$E_{m,n}$ (GPa)
26	0	37.6	0.25	4.8	4.8	4.8
	1	44.6	0.26	6.6	5.5	4.7
	3	60.6	0.27	6.4	6.2	5.4
	5	71.4	0.27	7.1	6.9	5.8
	7	85.6	0.28	7.3	7.6	6.3
	12	101.6	0.24	5.9	6.0	5.9
38	0	34.8	0.25	6.9	6.0	4.1
	1	42.2	0.26	7.3	6.1	4.4
	3	59.1	0.24	4.4	4.5	4.4
	5	70.0	0.26	5.3	5.2	5.0
	7	80.9	0.26	4.5	4.7	4.8
	12	97.6	0.27	6.7	6.5	6.0
51	0	30.9	0.22	3.4	3.7	2.5
	1	39.3	0.25	3.1	3.2	3.3
	3	54.6	0.25	5.8	4.7	3.5
	5	67.7	0.26	4.9	4.9	4.8
	7	75.0	0.22	5.1	5.1	4.7
	12	93.9	0.25	5.7	5.7	5.9
63	0	28.6	0.20	3.7	3.4	3.2
	1	37.6	0.24	3.3	4.0	4.1
	3	54.0	0.23	3.9	3.9	3.4
	5	63.7	0.25	3.8	3.2	3.5
	7	73.5	0.24	3.7	3.7	3.5
	12	89.2	0.26	4.8	4.8	4.6

**Table 4** Deformation moduli for case III

Joint frequency, $J_f$ (joints/m)	$\sigma_3$ (MPa)	$\sigma_1$ (MPa)	$\nu$	$E_{m,1}$ (GPa)	$E_{m,2}$ (GPa)	$E_{m,3}$ (GPa)
26	0	35.4	0.21	5.1	5.3	4.9
	1	41.9	0.21	5.3	6.2	4.7
	3	53.1	0.15	5.8	5.7	5.8
	5	66.3	0.20	4.9	4.3	5.6
	7	74.7	0.23	5.4	5.7	5.2
	12	90.7	0.28	5.9	5.7	6.1
38	0	32.9	0.22	4.2	4.3	4.5
	1	39.8	0.25	3.5	4.3	3.0
	3	50.0	0.26	3.9	5.2	3.1
	5	60.0	0.24	4.7	6.2	3.8
	7	69.9	0.26	4.5	4.0	5.1
	12	83.3	0.26	5.7	5.5	5.8
51	0	25.5	0.19	3.4	3.2	3.0
	1	34.7	0.16	2.3	3.6	1.7
	3	46.2	0.16	2.1	2.0	2.2
	5	56.7	0.17	2.6	2.8	2.5
	7	62.4	0.17	3.4	3.5	3.2
	12	74.4	0.23	3.9	4.5	4.4
63	0	20.4	0.20	3.0	2.9	2.8
	1	28.2	0.21	1.7	2.6	1.2
	3	41.1	0.17	2.8	3.0	2.7
	5	51.2	0.26	2.4	2.3	2.5
	7	57.0	0.19	2.2	2.1	2.2
	12	69.4	0.23	3.3	3.4	3.2
76	0	18.1	0.12	0.6	0.6	0.6
	1	25.3	0.15	0.9	1.1	0.7
	3	35.2	0.16	1.5	1.5	1.5
	5	44.4	0.22	1.6	1.6	1.5
	7	50.0	0.26	1.8	1.8	1.8
	12	62.2	0.29	2.2	2.2	2.2

joints normal to  $\sigma_1$  (Case II, Fig. 4b). For example, the strengths of the specimens in case I with 63 joints/m decreases by about 20 % from the intact strength. Under this joint frequency the specimen strengths for case II decrease by about 15 %. The effects of joint frequency are greatest for the three-joint set specimens (Case III, Fig. 4c). The strengths of specimens containing three-joint sets with 63 joints per meter drop by nearly 40 % from the intact strength.

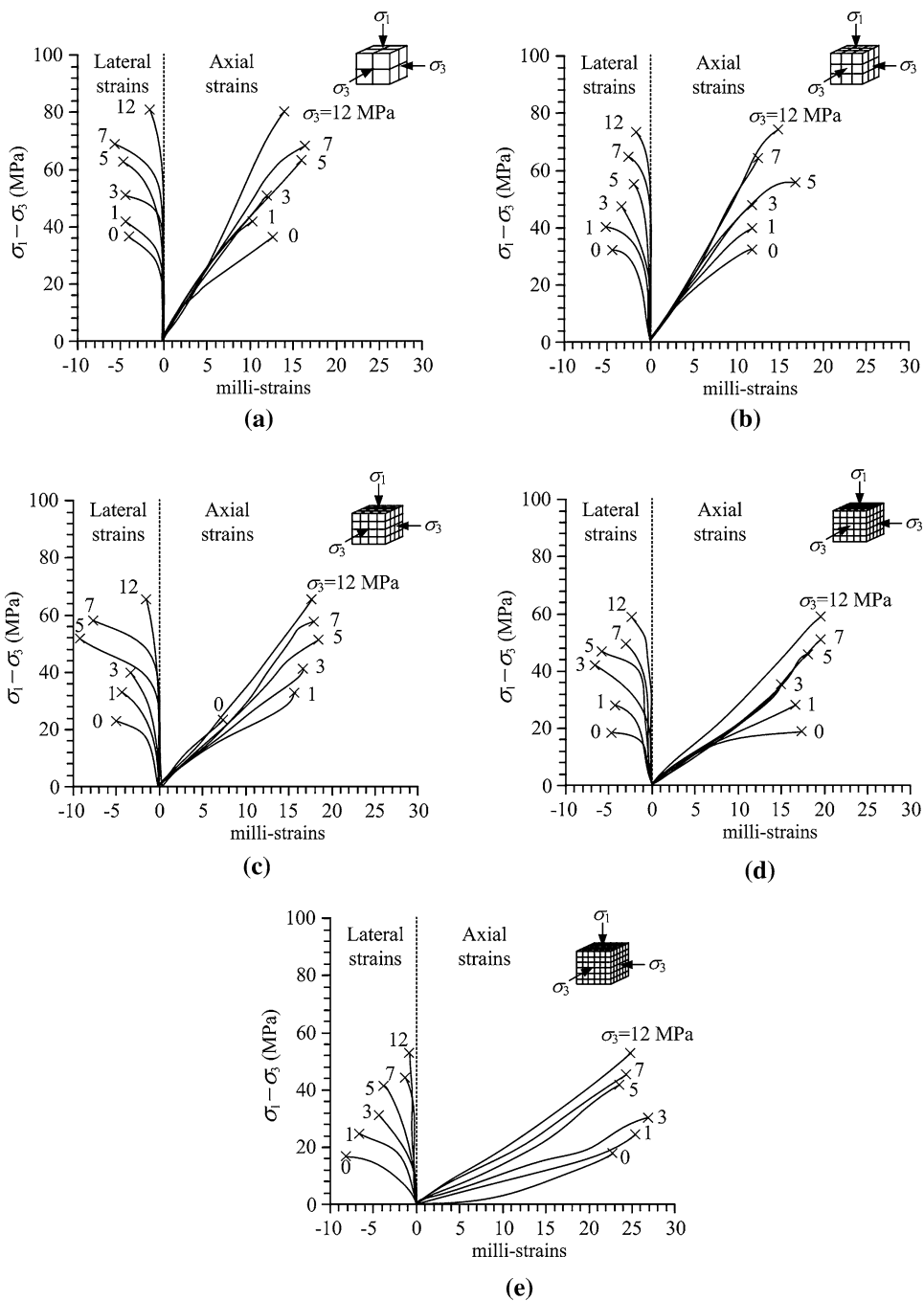
The decreases of the specimen strengths with increasing joint frequencies can also be observed from the  $\sigma_1$ - $J_f$  diagrams in Fig. 5. For the one-joint set specimens the differences of the strengths between case I and case II tend to be larger when the confining stresses increase (Fig. 5a). The  $\sigma_1$ - $J_f$  diagrams for case III (Fig. 5b) suggest also that the decreases of the three-joint set specimen strengths with increasing joint frequency are more rapid than those of the one-joint set specimens.

### Post-test observations

Post-test specimens show two types of failure mode: extensile splitting and compressive shear failure. The specimens with joints parallel to  $\sigma_1$  (Case I) failed mainly

under the extensile splitting mode, particularly under low confining stresses (Fig. 6a). Some shear fractures were found in the specimens that failed under high confining stresses. The compressive shear failure was predominant in the specimens with joints normal to  $\sigma_1$  (Case II, Fig. 6b). These observations support the measurement results that the single-joint set specimens with joints normal to  $\sigma_1$  (Case II) show higher strength than those with joints parallel to  $\sigma_1$  (Case I). The strength discrepancies are primarily due to the fact that  $\sigma_1$  direction for case I was parallel to small plates of the sandstone forming the rock mass models. The height-to-width ratios of these plates are relatively high (varying from 2 to 6, depending on the joint frequencies). Under axial loading, each plate can laterally dilate (toward the thinner sides), and hence the extensile fractures can be induced in vertical or nearly vertical directions. The pre-existing joints also help the induced

**Fig. 3** Examples of differential stresses as a function of strain for three mutually perpendicular joint sets under various confining pressures. **a** 26 joints/m, **b** 38 joints/m, **c** 51 joints/m, **d** 63 joints/m and **e** 76 joints/m



extensile fractures to propagate through the specimen models. The induced fractures can propagate more easily for the specimens with higher joint frequency, as compared to those with lower joint frequencies. This explains why the strengths of case I specimens decreased with increasing joint frequency. Under large confinement the lateral dilation of the sandstone plates toward the pre-existing joints becomes more difficult, and hence some shear fractures are induced across the specimen models.

The sandstone plates assembled for case II specimens were normal to the  $\sigma_1$  direction. They could not dilate easily under loading, and therefore the compressive shear fractures were predominant. As a result the strengths of case II specimens tended to be greater than those of case I. These shear fractures for case II can propagate more easily in specimens with higher joint frequencies and under lower confining stresses, as compared to those with lower joint frequencies and higher confining stresses.

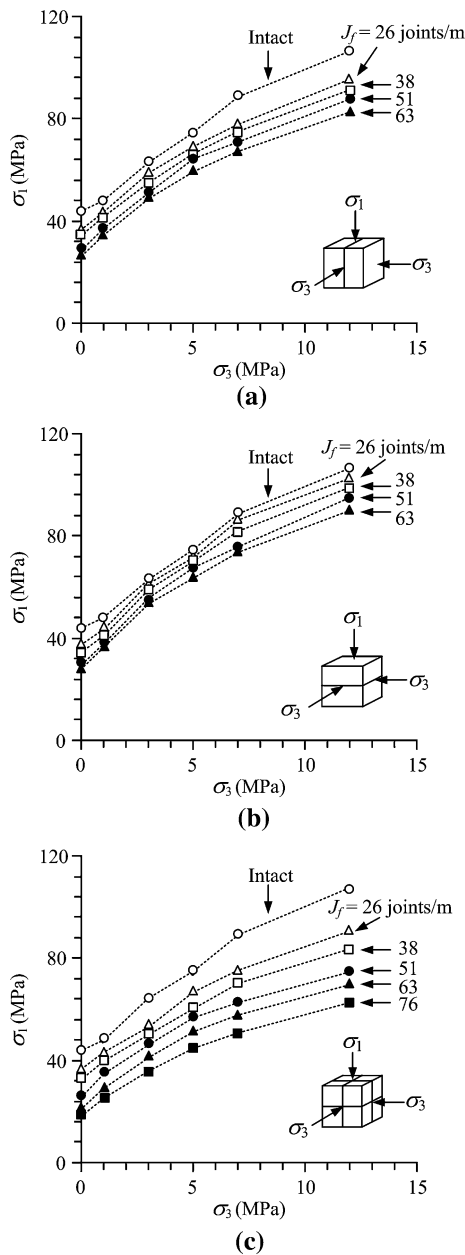


**Fig. 4** Major principal stresses at failure as a function of confining pressure for cases I (a), II (b), and III (c)

Both failure modes were found in the three-joint set specimens (Case III, Fig. 6c). This is probably because all case III specimens were formed by small cubical blocks of sandstone (varying from  $13 \times 13 \times 13$  to  $40 \times 40 \times 40$  mm<sup>3</sup>, depending on joint frequency). Under the same joint frequency the strengths of the case III specimens were lower than those of cases I and II because each sandstone block had an additional free face to dilate (i.e., there were two mutually perpendicular joint sets parallel to the  $\sigma_1$  direction).

For all cases the extensile splitting and shear fractures were induced in the intact portion of the specimens. This suggests that if there were invisible cracks or damages along the edges and corners of the small blocks, they may not have had a significant impact on the strength of the specimens.

### Strength criteria

Four commonly used strength criteria were compared against the test results obtained from the three-joint set specimens. These include criteria introduced by Hoek–Brown (1980), Sheorey (1989), Yudhbir et al. (1983), and Ramamurthy and Arora (1994). Exhaustive reviews of these criteria have been given elsewhere (Hoek and Brown 1980; Sheorey 1997; Hoek et al. 2002; Edelbro 2004). They have been widely used to study the strengths of rock mass.

The Hoek–Brown (1980) criterion defines the relationship between the major and minor principal stresses at failure as:

$$\sigma_1 = \sigma_3 + \sqrt{m\sigma_c\sigma_3 + s\sigma_c^2} \tag{1}$$

where  $m$  and  $s$  are material constants and  $\sigma_c$  is the uniaxial compressive strength of the intact rock.

Sheorey (1989) defines the rock mass strength criterion as:

$$\sigma_1 = \sigma_{cm} \left( 1 + \frac{\sigma_3}{\sigma_{tm}} \right)^{b_m} \tag{2}$$

where  $b_m$  is a constant,  $\sigma_{cm}$  is the uniaxial compressive strength of rock mass, and  $\sigma_{tm}$  is the uniaxial tensile strength of rock mass.

Yudhbir et al. (1983) modify the original Bieniawski (1974) criterion, and propose a more general form as:

$$\frac{\sigma_1}{\sigma_c} = A + B \left( \frac{\sigma_3}{\sigma_c} \right)^\alpha \tag{3}$$

where  $\alpha$  and  $B$  are material constants, and  $A$  is a dimensionless parameter depending on rock mass quality.

Ramamurthy and Arora (1994) present a strength criterion that is modified from the Mohr–Coulomb theory:

$$\frac{\sigma_1 - \sigma_3}{\sigma_3} = \beta \left( \frac{\sigma_{cm}}{\sigma_3} \right)^\alpha \tag{4}$$

where  $\alpha$  and  $\beta$  are the material constants. Ramamurthy and Arora (1994) suggest an alternative formula to determine  $\sigma_{cm}$  in terms of joint factor  $J_F$  as:  $\sigma_{cm} = \sigma_c \exp(-0.008 J_F)$ .

Hoek et al. (2002) propose a generalized form of the Hoek–Brown criterion as:

$$\sigma_1 = \sigma_3 + (m_b\sigma_c\sigma_3 + s\sigma_c^2)^a \tag{5}$$

**Fig. 5** Failure stress ( $\sigma_1$ ) as a function of joint frequency ( $J_f$ ) for one-joint set specimens (a) and three-joint set specimens (b)

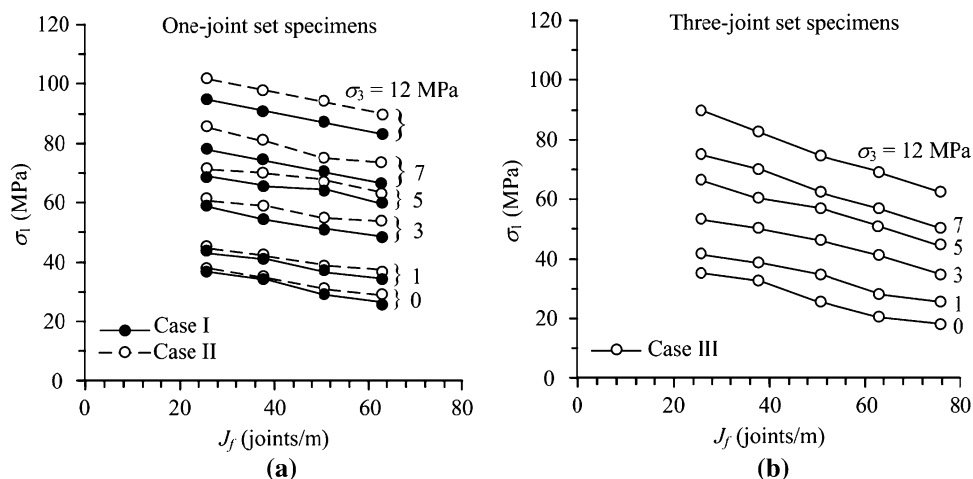
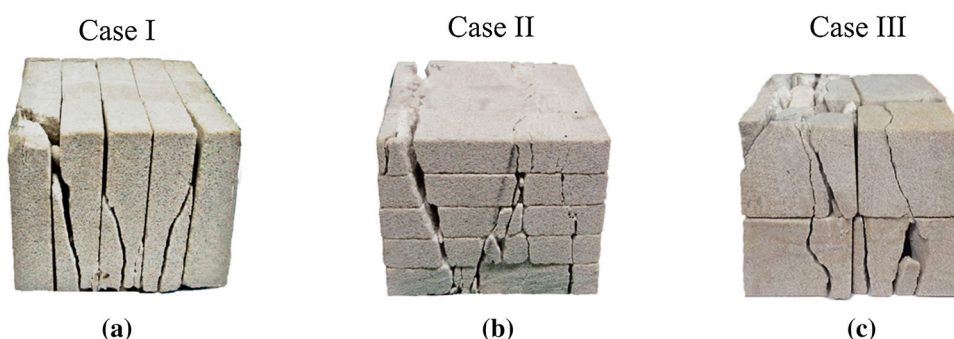


**Fig. 6** Examples of extensile splitting (a), compressive shear failure (b), and combination mode (c)

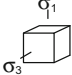
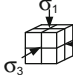
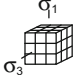
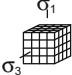
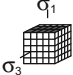
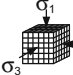


where  $m_b$ ,  $s$  and  $a$  are fitting parameters. It is applicable to a heavily jointed rock mass. The parameters  $m_b$  and  $s$  can be estimated from the geological strength index (GSI) (Hoek 1994; Hoek et al. 1995; Hoek and Brown 1998; Sonmez and Ulusay 1999). This index is determined from the joint surface conditions, structure rating, and volumetric joint count. The calculated GSI for the rock specimens used here are from 40 to 45 because the tested joints have no infilling and weathering. It is recommended that if GSI is greater than 25, the “ $a$ ” parameter should be set equal to 0.5 (Sheorey 1997; Sonmez and Ulusay 1999). In this study the original Hoek–Brown criterion is therefore used instead of the generalized Hoek–Brown criterion.

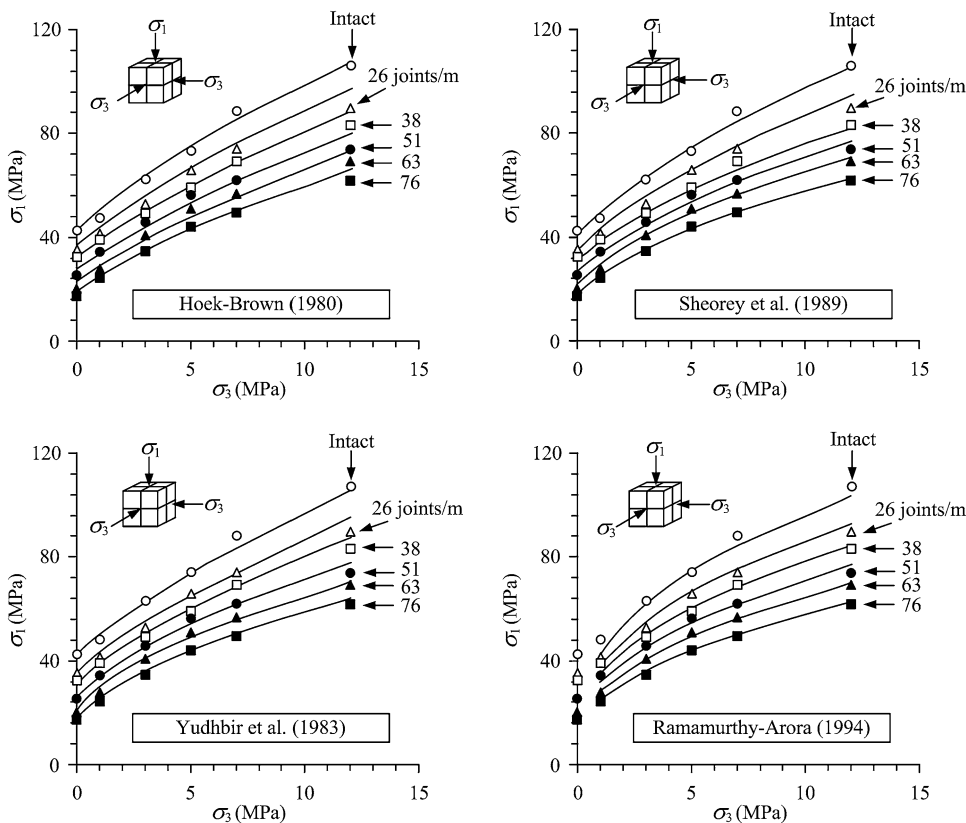
Statistical analyses are performed using the SPSS code (Wendai 2000) to fit the test results with the criteria above. The predictive capability of these criteria is determined and compared using the coefficient of correlation ( $R^2$ ) as an indicator. The material constants and coefficients of correlation calculated for these criteria are summarized in Table 5. All criteria provide good correlation with the test data, with  $R^2$  greater than 0.9. Figure 7 compares the test results with the curve fits in the terms of  $\sigma_1$  as a function of  $\sigma_3$  at failure.

Even though the Hoek and Brown criterion uses only two material constants, its predictive capability is as good as those with three material constants. Figure 8 shows the decrease of parameters  $m$  and  $s$  of the Hoek–Brown criterion as the joint frequency increases. For intact sandstone specimens, the parameter  $m$  is determined as 14.1 where  $s = 1.0$ . These  $m$  and  $s$  values for one-joint set specimens are greater than those for three-joint set specimens. For one-joint set specimens, the effect of joint orientation on  $m$  and  $s$  is relatively small (comparing cases I and II). The difference of the Hoek–Brown parameters between case I and case II seems to be the same for all joint frequencies (Fig. 8). However, significant decreases of both  $m$  and  $s$  values are found for the three-joint set specimens when the joint frequencies increase (Case III). The parameter  $s$  drops from 1.0 for intact condition to 0.1 for specimens with joint frequency of 76 joints/m. The Ramamurthy and Arora (1994) criterion can not predict the rock mass strength under unconfined conditions ( $\sigma_3 = 0$ ). As a result, Eq. (5) was proposed to predict the uniaxial strength of rock mass ( $\sigma_{cm}$ ). Both the Sheorey and Ramamurthy–Arora criteria can sufficiently describe the uniaxial strength of the rock specimens as shown in Fig. 9. The uniaxial strengths

**Table 5** Strength criteria and their constants calibrated from test results of case III

Strength criteria	Parameters	Joint frequencies (joints/m)					
		Intact	26	38	51	63	76
							
Hoek-Brown (1980) $\sigma_1 = \sigma_3 + (m \sigma_c \sigma_3 + s \sigma_c^2)^{1/2}$	$m$	14.10	11.30	9.22	7.89	6.03	4.83
	$s$	1.0	0.7	0.5	0.4	0.3	0.2
	$R^2$	0.992	0.969	0.984	0.971	0.979	0.986
Sheorey et al. (1989) $\sigma_1 = \sigma_{cm}(1 + \sigma_3/\sigma_{tm})^{b_m}$	$\sigma_{cm}$	41.8	35.8	31.0	26.5	22.9	19.6
	$\sigma_{tm}$	2.6	2.1	1.8	1.4	1.2	1.0
	$b_m$	0.54	0.51	0.48	0.47	0.46	0.45
	$R^2$	0.991	0.986	0.988	0.991	0.992	0.997
Yudhbir et al. (1983) $\sigma_1/\sigma_c = A + B(\sigma_3/\sigma_c)^\alpha$	$A$	0.97	0.82	0.70	0.59	0.50	0.43
	$B$	4.04	3.64	3.31	2.98	2.71	2.44
	$\alpha$	0.79	0.76	0.72	0.70	0.68	0.65
	$R^2$	0.986	0.984	0.986	0.987	0.989	0.993
Ramamurthy and Arora (1994) $(\sigma_1 - \sigma_3)/\sigma_3 = \beta(\sigma_{cm}/\sigma_3)^\alpha$	$\sigma_{cm}$	43.3	37.4	32.3	27.5	24.0	20.7
	$\beta$	3.19	3.15	3.13	3.08	3.00	2.90
	$\alpha$	0.69	0.69	0.69	0.69	0.69	0.69
	$R^2$	0.989	0.973	0.979	0.980	0.997	0.995

**Fig. 7** Test results (points) and curve fits for four strength criteria





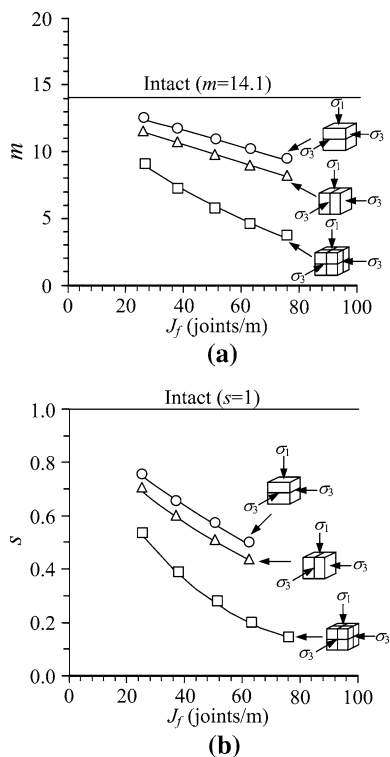


**Fig. 8** Hoek–Brown parameters *m* (a) and *s* (b) as a function of joint frequency

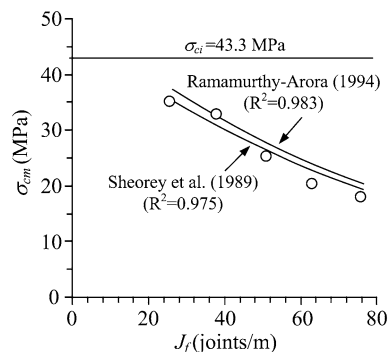


**Fig. 9** Uniaxial compressive strengths of rock mass model ( $\sigma_{cm}$ ) with three joint sets (case III) as a function of joint frequency. The predictions (lines) are compared with the measurements (points)

decrease from 43.3 MPa for intact conditions to about 20 MPa for the joint frequency of 76 joints/m.

**Deformation moduli**

The deformation moduli along the three principal axes of rock specimens are determined from the stress–strain curves at about 50 % of the failure stress. It is initially assumed that the Poisson’s ratio ( $\nu$ ) of the specimens is the same for all principal planes. The deformation moduli along the three principal

directions for each case can be derived from the elastic stress–strain relations (Jaeger et al. 2007) as shown below.

In case I:

$$\epsilon_{1,p} = \sigma_1/E_{m,p} - \nu(\sigma_3/E_{m,p} + \sigma_3/E_{m,n}) \tag{6}$$

$$\epsilon_{3,p} = \sigma_3/E_{m,p} - \nu(\sigma_1/E_{m,p} + \sigma_3/E_{m,n}) \tag{7}$$

$$\epsilon_{3,n} = \sigma_3/E_{m,n} - \nu(\sigma_1/E_{m,p} + \sigma_3/E_{m,p}) \tag{8}$$

Case II:

$$\epsilon_{1,n} = \sigma_1/E_{m,n} - \nu(\sigma_3/E_{m,p} + \sigma_3/E_{m,p}) \tag{9}$$

$$\epsilon_{3,p} = \sigma_3/E_{m,p} - \nu(\sigma_1/E_{m,n} + \sigma_3/E_{m,p}) \tag{10}$$

$$\epsilon_{3,p} = \sigma_3/E_{m,p} - \nu(\sigma_1/E_{m,n} + \sigma_3/E_{m,p}) \tag{11}$$

where  $\epsilon_{1,p}$  and  $\epsilon_{1,n}$  are the major principal strains parallel and normal to the joints,  $\epsilon_{3,p}$  and  $\epsilon_{3,n}$  are the minor principal strains parallel and normal to the joints, and  $E_{m,p}$  and  $E_{m,n}$ , are the deformation moduli parallel and normal to the joints.

In case III:

$$\epsilon_{1,m} = \sigma_1/E_{m,1} - \nu(\sigma_3/E_{m,2} + \sigma_3/E_{m,3}) \tag{12}$$

$$\epsilon_{3,m} = \sigma_3/E_{m,2} - \nu(\sigma_1/E_{m,1} + \sigma_3/E_{m,3}) \tag{13}$$

$$\epsilon_{3,m} = \sigma_3/E_{m,3} - \nu(\sigma_1/E_{m,1} + \sigma_3/E_{m,2}) \tag{14}$$

where  $\epsilon_{1,m}$  is the major principal strain,  $\epsilon_{3,m}$  is the minor principal strains,  $E_{m,1}$  is the deformation modulus along the vertical ( $\sigma_1$ ) axis, and  $E_{m,2}$  and  $E_{m,3}$  are the deformation moduli along the two lateral principal axes. Tables 2, 3, and 4 show the calculation results for all cases. The calculated Poisson’s ratios tend to be independent of the joint frequency and loading direction. Their values average between 0.23 and 0.29. For one-joint set specimens the deformation moduli parallel to the joints ( $E_{m,p}$ ) are about 13 % higher than those normal to the joints ( $E_{m,n}$ ) as shown in Fig. 10. This is true for all joint frequencies regardless of whether the joints are parallel (case I) or normal (case II) to  $\sigma_1$ . For the three-joint set specimens, the deformation moduli are similar for all principal directions (Fig. 11). Figure 12a and b plot the average deformation moduli that are parallel ( $E_{m,p}$ ) and normal ( $E_{m,n}$ ) to the joints for cases I and II. For the three-joint set specimens (case III), the deformation moduli averaged from the three principal directions (represented by  $E_m$ ) are plotted as a function of  $\sigma_3$  in Fig. 12c. The deformation moduli ( $E_{m,p}$ ,  $E_{m,n}$  and  $E_m$ ) decrease with increasing joint frequency.

**Deformability criteria**

The deformation moduli calculated above are compared against the criteria developed by Goodman (1970), Yoshinaka and Yamabe (1986), and Ramamurthy (2001).

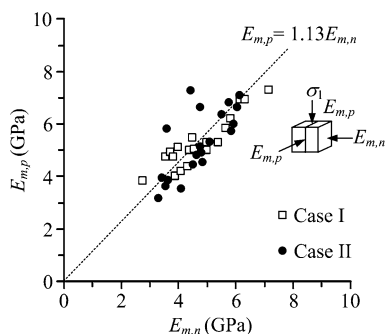


**Fig. 10** Deformation moduli parallel to joint planes as a function of those normal to joint planes

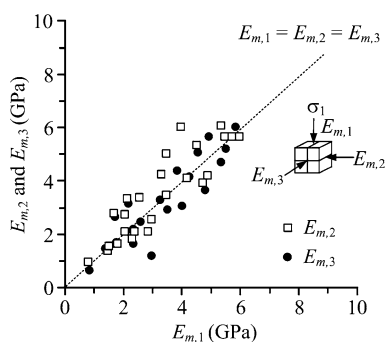


**Fig. 11** Deformation moduli calculated along the two minor principal axes ( $E_{m,2}$  and  $E_{m,3}$ ) as a function of those along the major principal axis ( $E_{m,1}$ ) for case III

Goodman (1970) presents an equation to determine the deformation modulus that is normal to the joints as:

$$\frac{1}{E_{m,n}} = \frac{1}{k_n s} + \frac{1}{E_i} \tag{15}$$

where  $E_i$  is the elastic modulus of intact rock,  $k_n$  is normal joint stiffness and  $s$  is the average joint spacing. This equation is only applicable to the results obtained from case II testing.

Yoshinaka and Yamabe (1986) proposed an equation to describe the deformability of samples with more than one joint under various joint orientations.

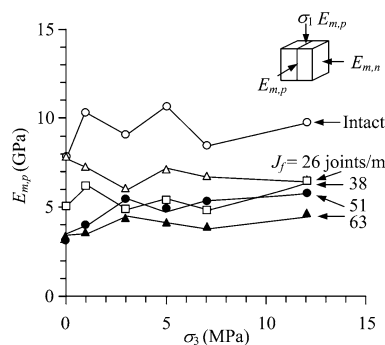
For case I testing, the joints are parallel to  $\sigma_1$  and the proposed equation becomes:

$$\frac{1}{E_{m,p}} = \frac{1}{E_i} \tag{16}$$

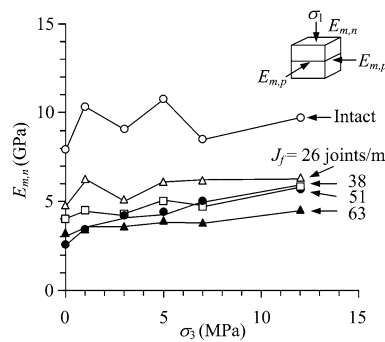
For cases II and III, the joints are parallel and normal to  $\sigma_1$  and their equations become:

$$\frac{1}{E_{m,n}} = \frac{1}{E_i} + \frac{1}{k_n s} \text{ (Case II)} \tag{17}$$

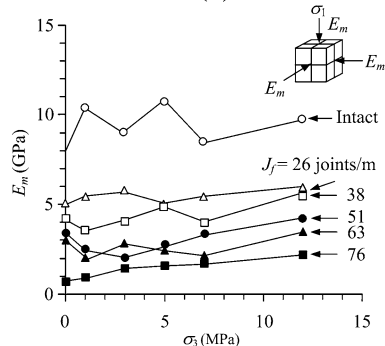
$$\frac{1}{E_m} = \frac{1}{E_i} + \frac{1}{k_n s} \text{ (Case III)}. \tag{18}$$



(a)



(b)



(c)

**Fig. 12** Deformation moduli parallel (a) and normal (b) to  $\sigma_1$  axis as a function of confining stress for one-joint set specimens and for three-joint set specimens (c)

Ramamurthy (2001) defines the relationship between the ratios of deformation moduli,  $E_{m,n}/E_i$ ,  $E_{m,p}/E_i$  and joint factor ( $J_F$ ) as:

$$E_{m,n} = E_{m,p} = E_i \exp(-1.15 \times 10^{-2} J_F) \tag{19}$$

where  $J_F$  is the joint factor, which is defined by:

$$J_F = \frac{J_f}{n \cdot r} \tag{20}$$

where  $J_f$  is the joint frequency (number of joints per meter),  $n$  is the inclination parameter depending upon the orientation of the joint, and  $r$  is a joint strength parameter dependent upon the joint condition. Note that Eqs. (19) and (20) are applicable to cases I and II only.

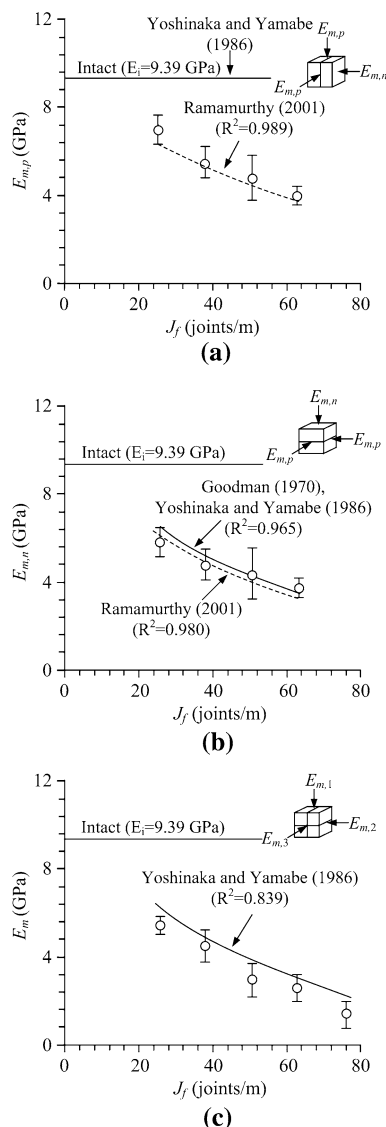


**Fig. 13** Predictions of deformation moduli compared with test data for one-joint set specimens (a, b) and three-joint set specimens (c). Points and error bars represent mean and standard deviation of deformation moduli from all confining pressures

The elastic moduli that are parallel and normal to the joints are plotted as a function of joint frequency for single-joint set specimens in Fig. 13a and b. Their average value (data point) and standard deviation (shown as error bars) obtained from all confining pressures are shown in the figure. The joint normal stiffness used here is 381.2 GPa/m, which is obtained from Kamonphet (2012). The elastic modulus of the intact sandstone in the figure is averaged from the measurement results given in Fig. 12. The joint factors of Ramamurthy (2001) used in this study are summarized in Table 6. The Ramamurthy (2001) equation gives a good estimation for the deformation moduli parallel to the joint planes (Fig. 13a) and normal to the joint planes (Fig. 13b). The Goodman (1970) and Yoshinaka and

**Table 6** Joint factors calculated for this study

Joint orientation	Joint frequency ( $J_f$ )	$n$	$r$	Joint factor ( $J_F$ )
One-joint set parallel to the major principal axis	Intact	1	0.8	–
	26	0.85	0.8	38.2
	38	0.85	0.8	55.9
	51	0.85	0.8	75.0
One-joint set normal to the major principal axis	Intact	1	0.8	–
	26	0.98	0.8	33.2
	38	0.98	0.8	48.5
	51	0.98	0.8	65.1
	63	0.98	0.8	80.4

Yamabe (1986) equations can also describe the deformation moduli normal to joint planes (Fig. 13b). Figure 13c shows the elastic moduli averaged from the three principal directions for the three-joint set specimens. Yoshinaka and Yamabe’s (1986) equation adequately describes the deformation moduli of the rock specimens with three-joint sets (Fig. 13c). Note that Yoshinaka and Yamabe (1986) cannot describe the deformation modulus of the rock mass along the axis that is parallel to the joint plane.

### Modified Goodman equation

The Goodman (1970) equation is modified here to determine the deformation modulus along three principal directions. It is proposed as:

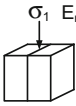
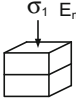
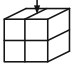
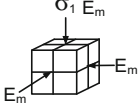
$$\frac{1}{E_m} = \frac{N}{k_n s} + \frac{1}{E_i} \tag{21}$$

Parameter  $N$  is introduced as an empirical constant to allow the Goodman equation to be able to predict the deformation moduli that are parallel to the joint plane (Table 7). The  $N$  values are defined by the direction of deformation moduli with respect to the joint plane as shown in Table 7. Predictions of the deformation moduli for the three cases are given in Fig. 14. Good correlations are obtained for all cases ( $R^2 > 0.9$ ). The proposed equation, however, can predict the deformation moduli only in the directions normal and parallel to the joint planes.

### Discussions and conclusions

Series of triaxial compression tests were performed to determine the strength and deformability of small-scale rock mass models with single- and multiple-joint sets and joint frequencies under large confinements. It was found that the compressive strengths decrease with increasing

**Table 7** Parameter  $N$  defined for the modified Goodman equation

Number of joint sets	Orientation of joint with respect to $\sigma_1$ axis	$N$
1	Parallel to $\sigma_1$ 	0.5 <sup>a</sup>
1	Normal to $\sigma_1$ 	1.0 (original Goodman's equation) <sup>a</sup>
2	Parallel and normal to $\sigma_1$ 	1.5
3	Two parallel and one normal to $\sigma_1$ 	2.0 <sup>a</sup>

<sup>a</sup> Verified by test results in Fig. 14

joint frequency. This agrees with the experimental observations by Ramamurthy and Arora (1994) on jointed specimens of Plaster of Paris. For one-joint set specimens tested here, the strengths of rock specimens with joints normal to the  $\sigma_1$  axis are always greater than those with joints parallel to the  $\sigma_1$  axis. This agrees with experimental observations by Colak and Unlu (2004), Saroglou and Tsiambaos (2008), and Goshtasbi et al. (2006). The decrease in rock mass strengths as the joint frequency increases tends to act equally throughout the range of confining stresses used here (1–12 MPa).

All strength criteria used here can sufficiently predict the strengths of the rock mass specimens under the confining stresses up to 12 MPa. The Hoek–Brown criterion with only two constants ( $m$  and  $s$ ) can describe the rock mass strengths as well as the three parameters criteria. The parameter  $s$  decreases rapidly with increasing joint frequency while parameter  $m$  tends to be insensitive to the joint frequency. The parameters  $m$  and  $s$  of the one-joint set specimens are higher than those of the three-joint set specimens. This suggests that decreasing joint set numbers will increase the rock mass strength. The measured uniaxial compressive strengths of the rock specimens ( $\sigma_{cm}$ ) decrease with increasing joint frequency. They agree well with the  $\sigma_{cm}$  calculated from the Sheorey (1989) and Ramamurthy and Arora (1994) criteria.

It is recognized that the joints studied here were simulated by smooth saw-cut surfaces. The strengths of the rock specimens for all cases, therefore, represent the lower bound of the strengths of actual rock mass where most fractures are rougher. In addition, the major principal stresses applied here are always normal or parallel to the

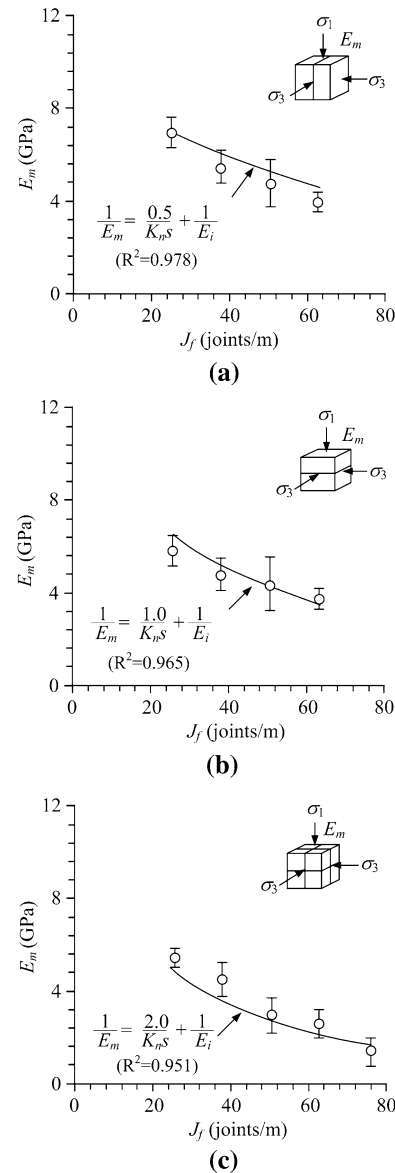


**Fig. 14** Predictions of deformation moduli by modified Goodman equation compared with test data for one-joint set specimens (a, b) and three-joint set specimens (c)

joint planes. It is expected that the rock mass model strengths would be lower if the applied stress makes oblique angles with the joint planes, as evidenced by the test results obtained by Ramamurthy and Arora (1994), Colak and Unlu (2004) and Goshtasbi et al. (2006).

For one-joint set specimens the deformation moduli parallel to the joints show the highest values compared to those that are normal to the joints. This is true for all joint frequencies. For three-joint set specimens, the deformation moduli are similar for all principal directions. The deformation moduli decrease with increasing joint frequency. This agrees with the experimental observations by Tiwari and Rao (2006).

The Goodman (1970) equation can sufficiently predict the deformation moduli for one-joint set specimens with joints normal to the major principal axis (case II). It, however, cannot calculate the deformation modulus for specimens with more than a one-joint set. Yoshinaka and Yamabe's (1986) equation can determine the specimen deformability with more than a one-joint set and orientation but it cannot calculate the deformation modulus parallel to the joints. Ramamurthy's (2001) equation can predict the deformation moduli parallel to the joint planes (case I) and normal to the joint planes (case II). It cannot calculate the deformation moduli of specimens with three-joint sets. A modified Goodman equation is proposed here to determine the deformation moduli along the three principal directions. The parameter  $N$  is introduced, whose values depend on joint set directions. The modified equation can adequately describe the deformation moduli parallel and normal to the joints planes for one-joint set and three-joint set specimens.

**Acknowledgments** This study was funded by the Suranaree University of Technology and by the Higher Education Promotion and National Research University of Thailand. Permission to publish this paper is gratefully acknowledged.

## References

- Bieniawski ZT (1974) Estimating the strength of rock materials. *J S Afr Inst Min Metall* 74:312–320
- Boonsener M, Sonpiron K (1997) Correlation of tertiary rocks in northeast, Thailand. *International Conference on Stratigraphy and Tectonic Evolution of Southeast Asia and the South Pacific*, Bangkok, Thailand, pp 656–661
- Cai M, Kaiser PK, Uno H, Tasaka Y, Minami M (2004) Estimation of rock mass deformation modulus and strength of jointed hard rock masses using the GSI system. *Int J Rock Mech Min Sci* 41(1):3–19
- Colak K, Unlu T (2004) Effect of transverse anisotropy on the Hoek-Brown strength parameter 'm<sub>i</sub>' for intact rocks. *Int J Rock Mech Min Sci* 41(6):1045–1052
- Ebadi M, Nasab SK, Jalalifar H (2011) Estimating the deformation modulus of jointed rock mass under multilateral loading condition using analytical methods. *J Min Environ* 2(2):146–156
- Edelbro C (2004) Evaluation of rock mass strength criteria. Dissertation, Lulea University of Technology
- Goodman RE (1970) The deformability of joints, determination of the in situ modulus of deformation of rock. ASTM STP 447, American Society for Testing and Materials, pp 174–196
- Goshtasbi K, Ahmadi M, Seyedi J (2006) Anisotropic strength behavior of slates in the Sirjan-Sanandaj zone. *J S Afr Inst Min Metall* 106:71–76
- Halakatevakis N, Sofianos AI (2010) Strength of a blocky rock mass based on an extended plane of weakness theory. *Int J Rock Mech Min Sci* 47:568–582
- Hoek E (1994) Strength of rock and rock masses. *ISRM News J* 2:4–16
- Hoek E, Brown ET (1980) Empirical strength criterion for rock masses. *J Geotech Eng Div ASCE* 160(GT9):1013–1035
- Hoek E, Brown ET (1998) Practical estimates of rock mass strength. *Int J Rock Mech Min Sci* 34:1165–1186
- Hoek E, Kaiser PK, Bawden WF (1995) Support of underground excavations in hard rock. Balkema, Rotterdam
- Hoek E, Carranza-Torres C, Corkum B (2002) Hoek-Brown failure criterion-2002 edition. *Proceedings of the fifth North American rock mechanics symposium*. Canada, Toronto, pp 267–273
- Jaeger JC, Cook NGW, Zimmerman RW (2007) *Fundamentals of rock mechanics*, 4th edn. Blackwell, Australia
- Kamonphet T (2012) Effect of cyclic loading peak shear strength of rock joints. Dissertation, Suranaree University of Technology
- Komonthammasopon S (2014) Effects of stress path on rock strength under true triaxial condition. Dissertation, Suranaree University of Technology
- Kulatilake PHS, Park J, Malama B (2006) A new rock mass failure criterion for biaxial loading conditions. *Geotech Geol Eng* 24:871–888
- Nasseri MHB, Rao KS, Ramamurthy T (2003) Anisotropic strength and deformational behavior of Himalayan schists. *Int J Rock Mech Min Sci* 40(1):3–23
- Rafiai H (2011) New empirical polyaxial criterion for rock strength. *Int J Rock Mech Min Sci* 48(6):922–931
- Ramamurthy T (2001) Shear strength response of some geological materials in triaxial compression. *Int J Rock Mech Min Sci* 38(5):683–697
- Ramamurthy T, Arora VK (1994) Strength predictions for jointed rocks in confined and unconfined states. *Int J Rock Mech Min Sci* 31(1):9–22
- Saroglou H, Tsiambaos G (2008) A modified Hoek-Brown failure criterion for anisotropic intact rock. *Int J Rock Mech Min Sci* 45(2):223–234
- Sheorey PR (1997) Empirical rock failure criterion. A.A.Balkema, Rotterdam
- Sheorey PR, Biswas AK, Choubey VD (1989) An empirical failure criterion for rocks and joint rock masses. *Eng Geol* 26(2):141–159
- Singh M, Singh B (2012) Modified Mohr-Coulomb criterion for non-linear triaxial and polyaxial strength of jointed rocks. *Int J Rock Mech Min Sci* 51:43–52
- Sonmez H, Ulusay R (1999) Modifications to the geological strength index (GSI) and their applicability to stability of slopes. *Int J Rock Mech Min Sci* 36:743–760
- Sridevi J, Sitharam TG (2000) Analysis of strength and moduli of jointed rocks. *Geotech Geol Eng* 18:3–21
- Tiwari R, Rao KS (2006) Deformability characteristics of a rock mass under true-triaxial stress compression. *Geotech Geol Eng* 24:1039–1063
- Wendai L (2000) Regression analysis, linear regression and profit regression, In 13 chapters; SPSS for Windows: statistical analysis. Publishing House of Electronics Industry, Beijing
- Yang ZY, Chen JM, Huang TH (1998) Effect of joint sets on the strength and deformation of rock mass models. *Int J Rock Mech Min Sci* 35(1):75–84
- Yoshinaka R, Yamabe T (1986) Joint stiffness and the deformation behaviour of discontinuous rock. *Int J Rock Mech Min Sci* 23(1):19–28
- Yudhbir Y, Lemanza W, Prinzl F (1983) An empirical failure criterion for rock masses. *Proc. Int. Congress Society of Rock Mechanics*, Melbourne, pp 1–8